

Formation and Ripening of Nanobelts/Nanofibers under Stirring of aqueous Solution – alternative models

Yaroslav Korol,¹ Andriy Gusak,¹ Marek Danielewski,² Marta Gajewska³

¹ Department of Physics, Cherkasy National University, Ukraine

² Faculty of Materials Science and Ceramics, AGH University of Science and Technology, Kraków, Poland

³ Academic Centre for Materials and Nanotechnology, AGH University of Science and Technology, Kraków, Poland

Corresponding author: Andriy Gusak, Department of Physics, Cherkasy National University, 81 Shevchenko blvd., Cherkasy, 18000, Ukraine, e-mail: amgusak@ukr.net

(received ..., accepted ...)

Abstract

Problem of V_2O_5 nanobelts production under intensive stirring of V_2O_5 powder in salted water is revisited. Method was initially proposed in 2016 but models and understanding were lacking. Here an independent attempt of the controlled V_2O_5 nanobelts formation and growth under stirring with various rotation frequencies is reported, as well as some alternative mechanisms and respective mathematical models of the nanobelts growth and ripening kinetics.

Keywords

Driven systems, fast diffusion, anisotropy, crystal growth, ballistic terms

1. Introduction

In this paper we discuss the very interesting and not well understood phenomena – production of strongly anisotropic structures in highly non-equilibrium open systems under intensive mechanical interference. In 2016 the new way of producing the long nanobelts of vanadium pentoxide V_2O_5 was suggested [1] – just by intensive stirring at room temperature of the initial oxide pentoxide powder in the salted water, for a few days. At that, the nanobelts appear and grow continuously at some places of the initial powder particles. Finally, powders transform into the array of very long (tens of microns) belts with cross-section of nanometric size. We tried to do some elementary modeling in this direction, [2-4], but the problem remains unsolved. Here we try

- 1) At least to reproduce experimentally the production algorithm and to find the governing parameters of this process,
- 2) To understand the possible physical reasons of nanobelts growth,



- 3) To suggest and discuss at least some simple alternative models.

Our article includes the following subtopics:

1. Our own experimental experience of V₂O₅ nanotube production at ambient by intensive stirring.
2. Two alternative mechanisms of nanobelt growth.
3. Anisotropy of nucleation-controlled crystallization.
 - 3.1. Velocity of nucleation-controlled crystallization in the fixed direction.
 - 3.2. Kinetic model of anisotropic layer-by layer growth.
4. Linear model of crystallization under stirring.
 - 4.1. Basic equations.
 - 4.2. Growth and ripening of anisotropic structures in open systems with ballistic events – qualitative analysis.

2. Experiment

First of all, we tried to reproduce the production of nanobelts according to receipts suggested in [1], but with own modifications. Our device provides the chosen, constant in time rotation frequency – Fig.1.

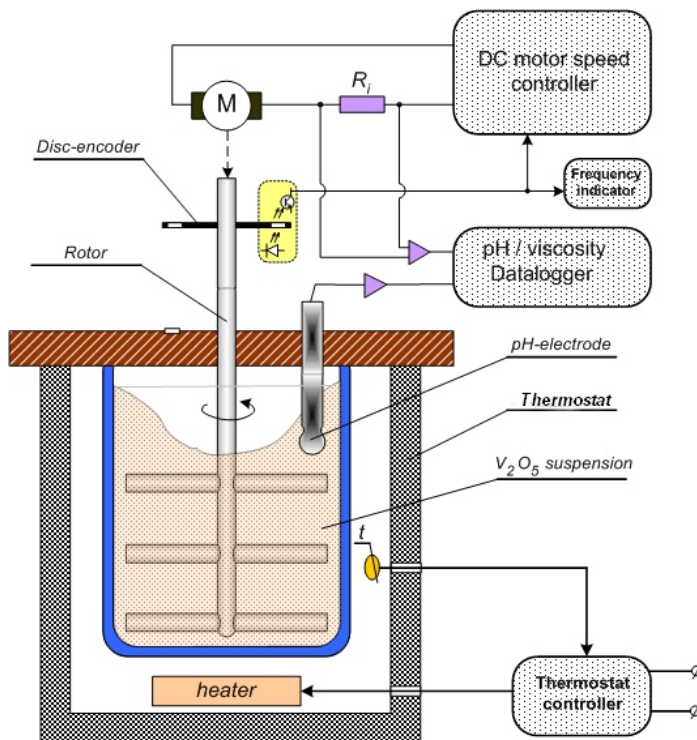


Fig. 1: Device for the synthesis of V₂O₅-nanocrystals

Since viscosity mainly increases in the course of stirring, the voltage providing the constant rotation velocity, automatically increases, and its dependence on time is measured. It gives the time dependence of viscosity. Simultaneously the time dependence of pH-index is measured. Constant temperature is automatically controlled with accuracy 1 degree. At Fig. 2 one may see the typical picture of the system after rotation was stopped and sedimentation occurred. (Here we don't have the full transformation of all powder into nanobelts). Red zone contains the product – nanosized vanadium pentoxide.



Fig. 2: Typical picture after 3 days of stirring and subsequent sedimentation. Upper (black) layer - NaCl+V₂O₅ - solution in water, red layer - V₂O₅-nano crystals, yellow layer – “semi-product”, bottom layer – untransformed V₂O₅ powder

History of transformations is following:

Fig. 3 is a SEM image of initial V₂O₅ powder. Individual powder particles have size about 100 microns and consist of agglomerated subcrystals of about 1 micron or few microns.

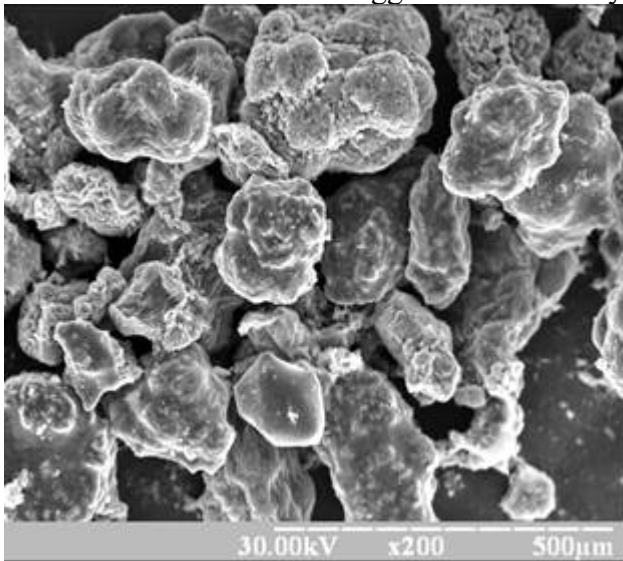


Fig. 3: Initial commercial powder (SEM image)

Fig. 4 demonstrates the initial stage of transformation. Surface of initial particles now is covered by kind of “moss” which we treat as nucleation and initial growth of filamentary nanocrystals of V₂O₅. Images were made at SEM in secondary electrons.

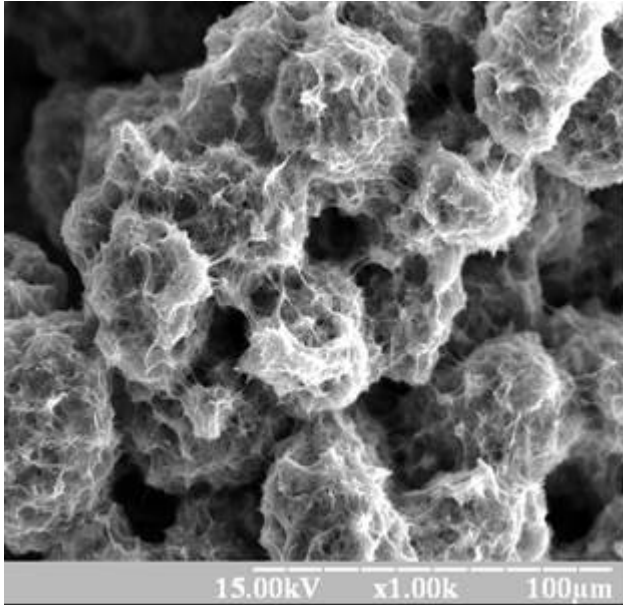


Fig. 4: Beginning of V_2O_5 –nanocrystals formation (covering by “moss”)

At Fig. 5 (SEM image in secondary electrons) one may observe the individual filamentary nanocrystals growing from the mother particle.

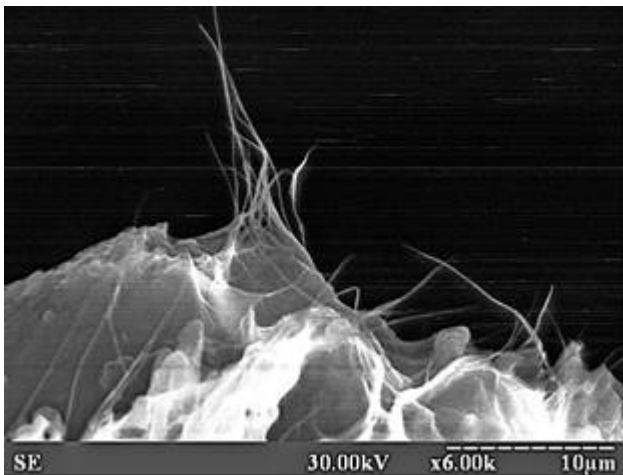


Fig. 5: Individual V_2O_5 –nanocrystals growing over the powder particle

At Fig.6 one may see an array of nanocrystals after consuming OF or being separated FROM the mother particles.

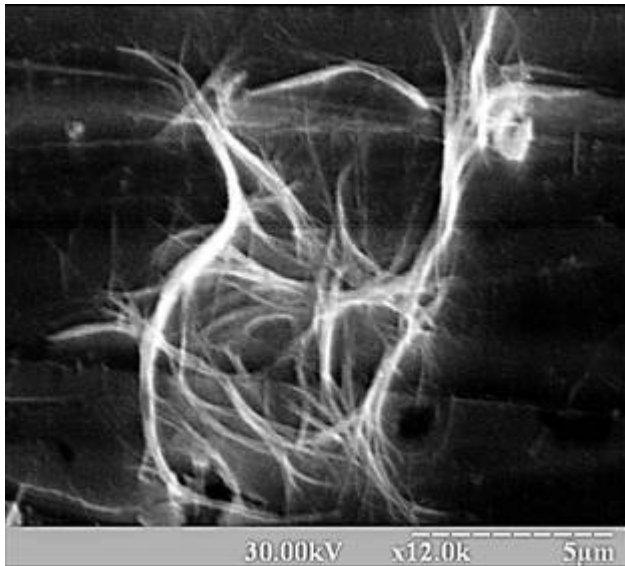


Fig. 6: The resulting V_2O_5 -nanofibers

In more details our samples were studied in the Centre for Materials and Nanotechnology of AGH University (Figs 7,8,9). At Fig.7a one may see the TEM image of the array of V_2O_5 nanocrystals. Fig. 7b is the TEM image of nanofibers.

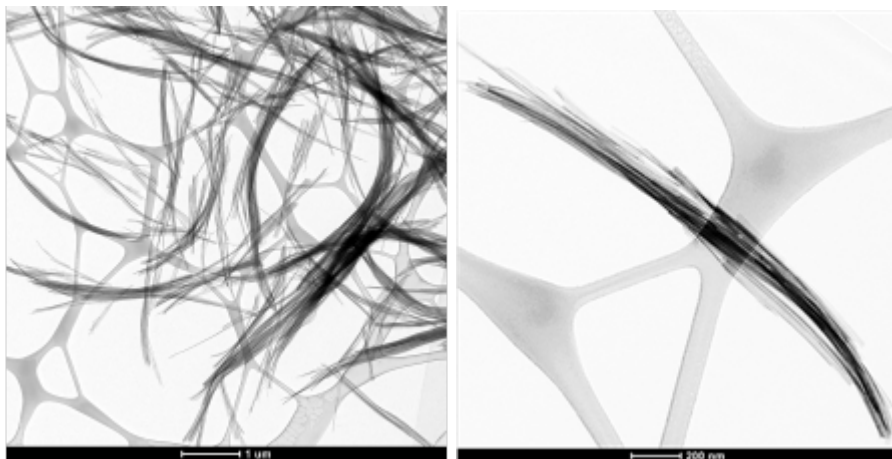


Fig. 7: Shape and fine structure of V_2O_5 arrays under high magnification (TEM images)

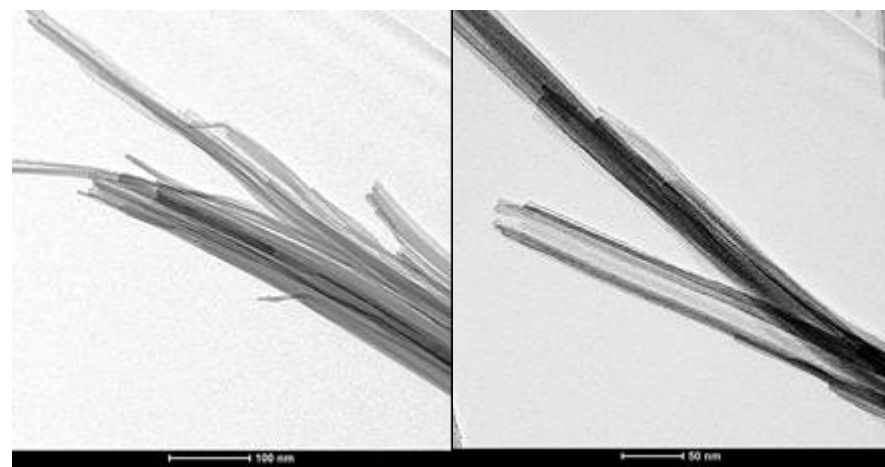


Fig. 8: Fine-structure of V_2O_5 nanocrystals

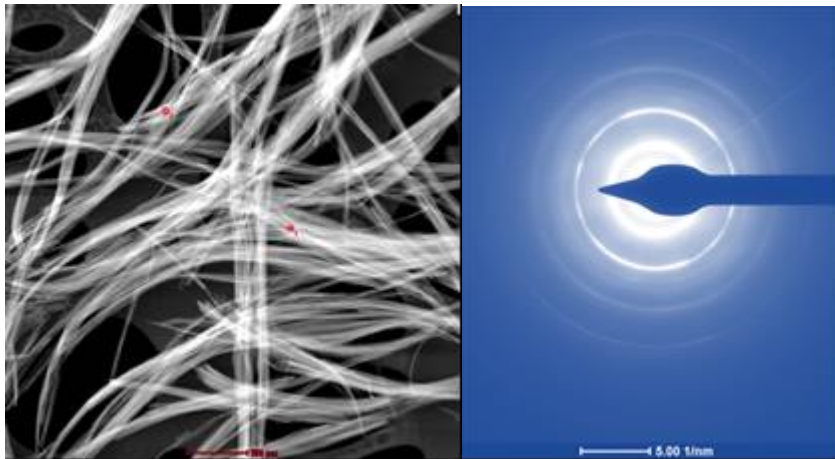


Fig. 9: STEM image of nanofibers array (a) and a Selected Area Electron Diffraction (SAED) from the area indicated by red circle at the left picture (b)

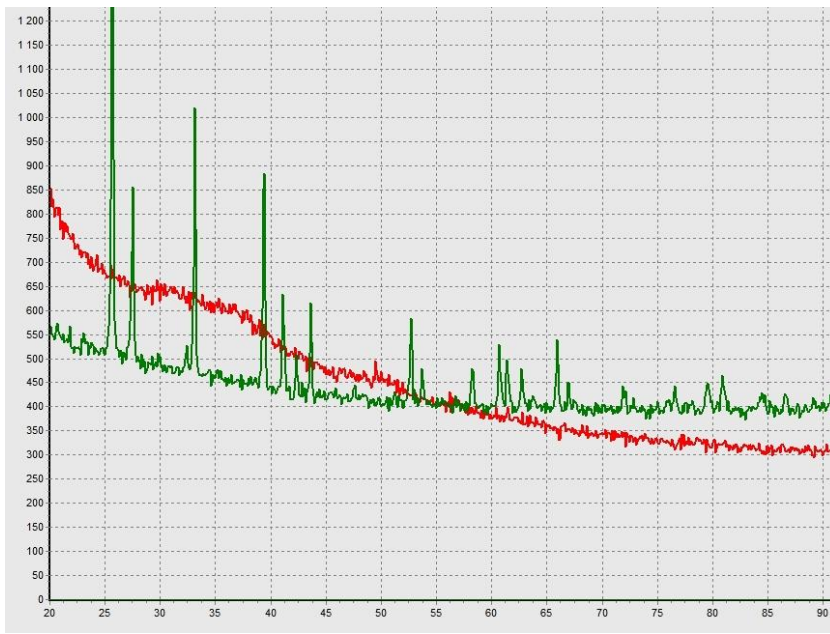


Fig. 10: XRD phase-analysis of V_2O_5 – nanocrystals. Green – initial powder, red – final nano-product.

Fig. 10 is a X-ray diffractogram (in iron -K-alpha radiation) of initial V_2O_5 powder and of the transformation product. As we can see, the diffractogram of the product does not contain characteristic peaks – most probably, due to thin cross-sections.

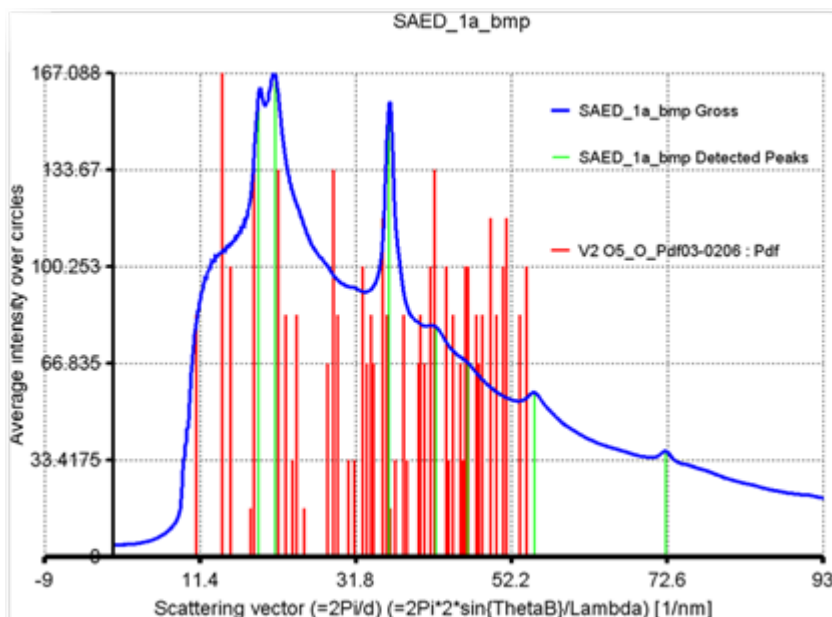


Fig. 11: SAED phase-analysis of V_2O_5 -nanocrystals

Fig. 11 is an attempt of phase analysis on the base of electron diffraction. Some observed peaks coincide with standard peaks.

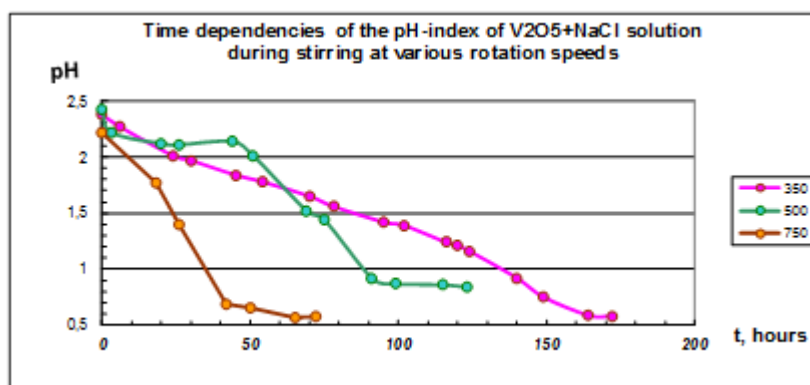


Fig. 12: Time dependencies of pH-value during V_2O_5 –nanophase formation for various rotation speeds (350, 500 and 750 rotations per minute)

Fig. 12 is a time dependence of pH-index in the process of rotation, at various rotation frequencies.

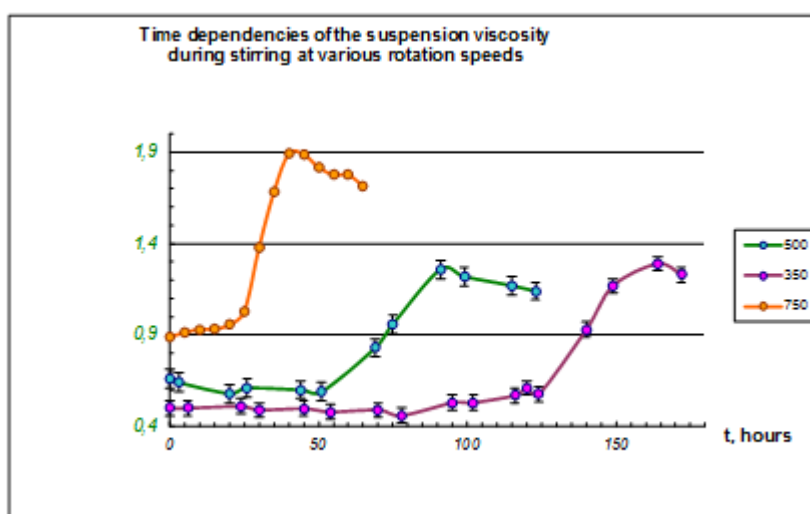


Fig. 13: Time dependencies of viscosity during V_2O_5 –nanophase formation for rotation speeds 350, 500 and 750 rotations per minute.

Fig. 13 is a time dependence of viscosity, also at various rotation frequencies.

3. Theoretical models

We suggest the first theoretic models of nanofibers formation by intensive stirring. Despite couple of published papers, we still don't know for sure the mechanism of nanobelts formation and growth. The published papers just demonstrate some possibilities. Namely, we still don't know for sure – is the nanobelts growth

- (A) just a „squeezing” from powder particles due to relaxation of stress or other accumulated defect energy, or
- (B) anisotropic nucleation-controlled crystallization via layer-by-layer growth,
- (C) the result of „atom-by-atom” recrystallization due to
- (C1) ballistic anisotropic erosion - detachment of ions from different faces due to intensive local irregular fluxes caused by stirring,
- (C2) fast diffusion/transfer of ions via the intermixed liquid medium from any facet of any nanobelt to any other facet of any other (or the same) nanobelt ,
- (C3) anisotropic thermal exchange (attachment/detachment) with liquid solution (with frequency obeying the Arrhenius law with activation energies depending on facet orientation).

3.1. Mechanism A: Squeezing” from powder particles due to relaxation of stress or other accumulated defect energy.

Concerning possibility (A), we just remind that typical whiskers, say, of tin are squeezed through the defect places of native oxide - they relax the stress, accumulated due to chemical reactions – say, solid-state reaction Cu plus Sn leading to formation of intermetallic compounds with very different atomic volume in comparison with volume of initial elements. In case of possibility A, one could assume that the commercial powder is in a highly non-equilibrium state and has a large amount of defect energy, accumulated during its production. Moreover, this defect energy may be increased due to intensive stirring of the powders. On the other hand, in this case (case of “squeezing”) system does not need any transfer of ions via the solution – on the other hand, we clearly observe the change of color which means dissolution of ions VO_2 in the water. Also, the time evolution of pH-index also demonstrates the production of extra H^+ -ions due to reaction $V_2O_5 + H_2O \rightarrow 2HVO_3$ and subsequent dissociation of HVO_3 into ions H^+ and VO_3^- . Thus, so far, we consider the “squeezing” mechanism as less probable.

3.2. Mechanism B: Anisotropic nucleation-controlled crystallization

Crystalline structure of V_2O_5 is orthorhombic so that the growth velocity in three different crystallographic directions (a-<010>, b-<001> and c-<100>) are expected to be different. Assume that each facet of the nanobelt moves into liquid solution by the nucleation-controlled layer-by-layer mechanism: each new layer waits for nucleation of rectangular nucleus. As shown in [1], the heights h_i of one-layer nuclei can be taken as $h_1 = 1.78$, $h_2 = 4.41$, and $h_3 = 5.85 \text{ \AA}$ for $V_2O_5(010)$, $V_2O_5(001)$, and $V_2O_5(100)$ surfaces, respectively. Let us assume that the spreading period after nucleation of overcritical 2D-island is much shorter than the waiting time of successful nucleation. Then the velocity of i-th facet propagation is equal to

$$v_i = h_i \times v_i \times S_i, \quad i=1 \text{ (facet (010)), } i=2 \text{ (facet (001)), } i=3 \text{ (facet (100))} \quad (1)$$

Here $S_1 = b * c, S_2 = c * a, S_3 = a * b$ - the area of corresponding facet, v_i is a probability per unit time per unit area of i-th facet to create the overcritical (viable) 2D-island. According to the Classical Nucleation Theory (CNT), nucleation frequency is a product of Zeldovich factor and the exponent of nucleation saddle-point value of Gibbs free energy change divided by $-kT$.

$$v_i = Z_i * \exp\left(-\frac{\Delta G_{crit}}{kT}\right). \quad (2)$$

Let the 2D nucleus be the rectangle of elementary height h and lateral sizes b and c . Let γb is a surface tension of the side facet $b * h$, γc is a surface tension of the side facet $c * h$. $\Delta\mu$ is a bulk driving force of crystallization per monomer. Let $S = b * c$ is an area of top surface of the nucleus, $\varphi = c/b$ is a shape factor, so that

$$S = b^2 \varphi, b = \sqrt{S/\varphi}, c = \sqrt{S * \varphi}. \quad (3)$$

Then

$$\begin{aligned} \Delta G(b, c) = \Delta G(S, \varphi) &= -\frac{h * b * c}{\Omega} * \Delta\mu + 2 * (\gamma b * b * h + \gamma c * c * h) = \\ &= h * \left(-\frac{S}{\Omega} * \Delta\mu + 2 * \sqrt{S}(\gamma b/\sqrt{\varphi} + \gamma c * \sqrt{\varphi})\right) \end{aligned} \quad (4)$$

Optimization (minimization) of Gibbs free energy over shape factor at fixed area S gives

$$\varphi_{opt} = \gamma b / \gamma c. \quad (5)$$

Substituting optimal shape factor into eq. (4), one gets:

$$\Delta G(S, \varphi_{opt}) = h * \left(-\frac{S}{\Omega} * \Delta\mu + 4 * \sqrt{\gamma b * \gamma c * S}\right). \quad (6)$$

Saddle-point is found from the condition of zero derivative over S :

$$\frac{1}{\Omega} * \Delta\mu = 2 * \sqrt{\gamma b * \frac{\gamma c}{S}} \Rightarrow \sqrt{S_{crit}} = 2 * \Omega \sqrt{\gamma b * \gamma c} / \Delta\mu. \quad (7)$$

$$\Delta G_{crit} = h * \left(4 * \Omega * \frac{\gamma b * \gamma c}{\Delta\mu}\right) = \frac{h}{\gamma a} * \left(4 * \Omega * \frac{\gamma a * \gamma b * \gamma c}{\Delta\mu}\right). \quad (8)$$

It means the following nucleation barriers of the layer-by-layer growth of three facets:

$$\Delta G_{crit}(010) = \frac{h(010)}{\gamma(010)} * \left(4 * \Omega * \frac{\gamma a * \gamma b * \gamma c}{\Delta\mu}\right),$$

$$\Delta G_{crit}(001) = \frac{h(001)}{\gamma(001)} * \left(4 * \Omega * \frac{\gamma a * \gamma b * \gamma c}{\Delta\mu}\right),$$

$$\Delta G_{crit}(010) = \frac{h(010)}{\gamma(010)} * \left(4 * \Omega * \frac{\gamma a * \gamma b * \gamma c}{\Delta\mu}\right)$$

$$\frac{da}{dt} = v_{010} = h_{010} * Z_{010} * \exp\left(-\frac{h(010)}{\gamma(010)} * \left(4 * \Omega * \frac{\gamma a * \gamma b * \gamma c}{kT * kT \ln\left(\frac{C}{C_{eq}}\right)}\right)\right) * b * c \quad (9a)$$

$$\frac{db}{dt} = v_{001} = h_{001} * Z_{001} * \exp\left(-\frac{h(001)}{\gamma(001)} * \left(4 * \Omega * \frac{\gamma a * \gamma b * \gamma c}{kT * kT \ln\left(\frac{C}{C_{eq}}\right)}\right)\right) * c * a \quad (9b)$$

$$\frac{dc}{dt} = v_{100} = h_{100} \times Z_{100} * \exp \left(-\frac{h(100)}{\gamma(100)} * \left(4 * \Omega * \frac{\gamma a * \gamma b * \gamma c}{kT * kT \ln \left(\frac{C}{C_{eq}} \right)} \right) \right) \times a * b \quad (9c)$$

All three surface tensions for three facets (010), (001) and (100) are not far from each other (about 0.5 J/m²), but the height of 2D atomic layer differ significantly [1]: $h(010) = 1.78 \text{ \AA}$, $h(001) = 4.41 \text{ \AA}$, $h(100) = 5.85 \text{ \AA}$.

$$\frac{ada}{bdb} = \frac{(h_{010} * Z_{010})}{(h_{001} * Z_{001})} * \exp \left(-\left(\frac{h(010)}{\gamma(010)} - \frac{h(001)}{\gamma(001)} \right) * \left(4 * \Omega * \frac{\gamma a * \gamma b * \gamma c}{kT * kT \ln \left(\frac{C}{C_{eq}} \right)} \right) \right)$$

It means that, for the late stage (when initial conditions are forgotten), the ratio of sides, for example, a and b, tends to

$$\frac{a}{b} = \sqrt{\frac{h_{010} Z_{010}}{h_{001} Z_{001}}} * \exp \left(-\left(\frac{h(010)}{\gamma(010)} - \frac{h(001)}{\gamma(001)} \right) * \left(2 * \Omega * \frac{\gamma a * \gamma b * \gamma c}{kT * kT \ln \left(\frac{C}{C_{eq}} \right)} \right) \right) = const \quad (10)$$

This expression is very sensitive to the supersaturation which appears to be a key parameter in this type of model. So far, we are not able to predict the dependence of supersaturation on the rotation frequency.

3.3. Mechanism C: Recrystallization in the driven system.

Model of layer-by-layer nucleation-controlled crystallization would be OK for the case of atomically flat facets. It is very hard to imagine atomically flat facets under 72 hours of intensive stirring. In this case atom-by-atom model [2] looks more reasonable than layer-by-layer model. Now we try a model of linear type: First, in this second model the velocity crystallization front for fixed facet of the rectangular crystal ($b*c$, $c*a$ or $a*b$) contains the term, proportional to supersaturation (in terms of chemical potentials) with different Onsager coefficients. Second, in this model the velocity contains the second (ballistic) anisotropic negative term proportional to stirring intensity and physically meaning an anisotropic erosion which is not thermal but instead driven by external factors (even at zero temperature):

$$\begin{cases} \frac{da}{dt} = 2L_a(\mu^{liq} - \mu_{bc}^{cryst}) - 2U_a \\ \frac{db}{dt} = 2L_b(\mu^{liq} - \mu_{ca}^{cryst}) - 2U_b \\ \frac{dc}{dt} = 2L_c(\mu^{liq} - \mu_{ab}^{cryst}) - 2U_c \end{cases} \quad (11a,b,c)$$

Elementary atomistic derivation of such kind of equations, on the base of atom-by-atom model, is simple and can be found in [2]. Ballistic (athermal, non-Arrhenius) velocities U are introduced as a development of George Martin's concept of so-called "ballistic events" in the driven systems [5].

Now we remind some elementary concepts of anisotropy related to different surface tensions at different facets of anisotropic crystal. Adding of some additional layer da over the side surface b-c increases the two side areas a-b by $2b*da$ and corresponding surface energy by $2\gamma_{ab}bda$, also it increases two side areas a-c by $2c*da$ and corresponding surface energy by $2\gamma_{ca}cda$. For calculation of the chemical potential of the side area 'b-c' we calculate the change of bulk Gibbs energy plus the changes of both surface energies, and divide all this by the number of atoms in the added cylindrical slice. We get the size effect for chemical potential.

$$\mu_{bc}^{cryst} = \frac{\partial G}{\partial N} = \frac{\mu_{bulk}^{cryst} \frac{bcda}{\Omega} + 2\gamma_{ab}bda + 2\gamma_{ca}cda}{\frac{bcda}{\Omega}} = \mu_{bulk}^{cryst} + \frac{2\gamma_{ab}\Omega}{c} + \frac{2\gamma_{ca}\Omega}{b} \quad (12a)$$

$$\mu_{ca}^{cryst} = \mu_{bulk}^{cryst} + \frac{2\gamma_{bc}\Omega}{a} + \frac{2\gamma_{ab}\Omega}{c} \quad (12b)$$

$$\mu_{ab}^{cryst} = \mu_{bulk}^{cryst} + \frac{2\gamma_{ca}\Omega}{b} + \frac{2\gamma_{bc}\Omega}{a} \quad (12c)$$

In equilibrium, when chemical potentials of both surfaces should be equal one gets the famous Wulff's rule

$$\frac{\gamma_{bc}}{a} = \frac{\gamma_{ca}}{b} = \frac{\gamma_{ab}}{c}, \text{ or, in other terms, } bc\gamma_{bc} = ca\gamma_{ca} = ab\gamma_{ab}. \quad (13)$$

Actually, the observed strong deviation from this rule stimulates our present modeling. Let us, once more, comment on the physical sense of kinetic equations (11). They contain thermal (quasi-equilibrium) term and ballistic term (clearly the term which perturbs the quasi-equilibrium). Thermal term in the expression for velocity is proportional to the difference of chemical potentials in solution and at the corresponding surface of the crystal. In case of "no stirring", the velocity is just the product of corresponding Onsager coefficient and of the difference of chemical potentials. Coefficients L_a, L_b and L_c are different (and can be very different – by orders of magnitude - at low temperatures due to Arrhenius law for the frequency of thermal detachments/attachments), and this is one of the possible sources of growth anisotropy. Second terms in both equations for velocities reflects our understanding of George Martin's idea of ballistic jumps. We assume that stirring may lead only to additional erosion (different for different facets), and the velocity of this erosion is proportional to the stirring intensity. Difference of ballistic erosion velocities is a second possible source of anisotropy.

Contrary to previous model, we will consider the cases of rather small supersaturation, so that

$$kT \ln \left(\frac{C}{C_{eq}} \right) = kT \ln \left(1 + \frac{C - C_{eq}}{C_{eq}} \right) \approx kT * \frac{C - C_{eq}}{C_{eq}} = kT * \frac{X - X_{eq}}{X_{eq}} = kT * \frac{\Delta}{X_{eq}} \quad (14)$$

Here X is a renormalized concentration in the liquid solution: $X = C/C_{solid}$ (C - number of monomers per unit volume of liquid, C_{solid} – number of monomers per unit volume of solid oxide. Then eqs. (11) transform into

$$\begin{cases} \frac{da}{dt} = \frac{2L_a kT}{x_{eq}} \left(\Delta - \frac{2x_{eq}\Omega}{kT} \left(\frac{\gamma_{ab}}{c} + \frac{\gamma_{ca}}{b} \right) - \frac{x_{eq} U_a}{kT L_a} \right), \\ \frac{db}{dt} = \frac{2L_b kT}{x_{eq}} \left(\Delta - \frac{2x_{eq}\Omega}{kT} \left(\frac{\gamma_{bc}}{a} + \frac{\gamma_{ab}}{c} \right) - \frac{x_{eq} U_b}{kT L_b} \right), \\ \frac{dc}{dt} = \frac{2L_c kT}{x_{eq}} \left(\Delta - \frac{2x_{eq}\Omega}{kT} \left(\frac{\gamma_{ca}}{b} + \frac{\gamma_{bc}}{a} \right) - \frac{x_{eq} U_c}{kT L_c} \right) \end{cases} \quad (15)$$

These equations are applied to all crystals- parallelepipeds (if crystal is still connected with its original “parent” – powder particle and grows preferentially along long side “a”, then factor 2 in the equation for da/dt should be changed to factor 1 -growth only from one side.)If one may imagine the array of all particles as the array of parallelepipeds (number of which changes with time), then the constraint of matter conservation is automatically provided by the equation

$$\begin{aligned} & (x_{eq} + \Delta(t)) \left(1 - \frac{\sum_i^{N(t)} a_i b_i c_i}{V^{tot}} \right) + \frac{\sum_i^{N(t)} a_i b_i c_i}{V^{tot}} = \\ & = (x_{eq} + \Delta(t=0)) \left(1 - \frac{\sum_i^{N(0)} a_{i0} b_{i0} c_{i0}}{V^{tot}} \right) + \frac{\sum_i^{N(0)} a_{i0} b_{i0} c_{i0}}{V^{tot}} \end{aligned} \quad (16)$$

For further analysis, it is convenient to introduce the characteristic lengths of the process, and nondimensional parameters – nondimensional time, nondimensional sizes (diameter and length) of the particles, nondimensional stirring factor, etc:

$$\begin{cases} \lambda_0 = x_{eq} \frac{2(\gamma_{bc}\gamma_{ca}\gamma_{ab})^{1/3}\Omega}{kT}, \tilde{V}^{total} = V^{total}/(\lambda_0)^3 \\ r_a^{therm} = \frac{\gamma_{bc}}{(\gamma_{bc}\gamma_{ca}\gamma_{ab})^{1/3}}, r_b^{therm} = \frac{\gamma_{ca}}{(\gamma_{bc}\gamma_{ca}\gamma_{ab})^{1/3}}, r_c^{therm} = \frac{\gamma_{ab}}{(\gamma_{bc}\gamma_{ca}\gamma_{ab})^{1/3}}, \\ r_a^{kinet} \equiv \frac{L_a}{(L_a L_b L_c)^{1/3}}, r_b^{kinet} \equiv \frac{L_b}{(L_a L_b L_c)^{1/3}}, r_c^{kinet} \equiv \frac{L_c}{(L_a L_b L_c)^{1/3}} \\ r_a^{bal} \equiv \frac{U_a}{(U_a U_b U_c)^{1/3}}, r_b^{bal} \equiv \frac{U_b}{(U_a U_b U_c)^{1/3}}, r_c^{bal} \equiv \frac{U_c}{(U_a U_b U_c)^{1/3}} \\ J \equiv \frac{x_{eq}(U_a U_b U_c)^{1/3}}{kT(L_a L_b L_c)^{1/3}} \\ \tau \equiv (L_a L_b L_c)^{1/3} \frac{2kT}{\lambda_0 x_{eq}} t, A \equiv \frac{a}{\lambda_0}, B \equiv \frac{b}{\lambda_0}, C \equiv \frac{c}{\lambda_0} \end{cases} \quad (17)$$

Respectively, we reformulate the kinetic equations and constraint of matter conservation in the simplest mathematical form.

$$\begin{cases} \frac{dA}{d\tau} = r_a^{kinet} \left(\Delta - \frac{r_c^{therm}}{C} - \frac{r_b^{therm}}{B} - \frac{r_a^{bal}}{r_a^{kinet} J} \right) \\ \frac{dB}{d\tau} = r_b^{kinet} \left(\Delta - \frac{r_a^{therm}}{A} - \frac{r_c^{therm}}{C} - \frac{r_b^{bal}}{r_b^{kinet} J} \right) \\ \frac{dC}{d\tau} = r_c^{kinet} \left(\Delta - \frac{r_a^{therm}}{A} - \frac{r_b^{therm}}{B} - \frac{r_c^{bal}}{r_c^{kinet} J} \right) \end{cases} \quad (18)$$

$$\begin{aligned} & (x_{eq} + \Delta(t)) \left(1 - \frac{\sum_i^{N(t)} A_i B_i C_i}{\tilde{V}^{total}} \right) + \frac{\sum_i^{N(t)} A_i B_i C_i}{\tilde{V}^{total}} = \\ & = (x_{eq} + \Delta(t=0)) \left(1 - \frac{\sum_i^{N(0)} A_{i0} B_{i0} C_{i0}}{\tilde{V}^{total}} \right) + \frac{\sum_i^{N(0)} A_{i0} B_{i0} C_{i0}}{\tilde{V}^{total}} \end{aligned} \quad (19)$$

At the stage of nucleation and independent growth only set of three equations (18) should be solved independently on other particles. At the ripening stage all facets of all particles

become interconnected by the matter conservation, and we should solve the set of $2N+1$ equations, where N is a number of particles which also changes with time.

We already know that at the stage of independent growth, when the supersaturation is kept almost constant, a strong anisotropy may be provided by the ratio $L_a/L_b \gg 1$ and $L_a/L_c \gg 1$. Yet, one more interesting possibility of strong anisotropy at the ripening stage may be related to anisotropy of ballistic terms. To understand this, let us, at first, consider a fully isotropic case of eqs. (18):

$$r_a^{kinet} = r_b^{kinet} = r_c^{kinet}, r_a^{therm} = r_b^{therm} = r_c^{therm}, r_a^{bal} = r_b^{bal} = r_c^{bal}$$

Then for all particles $A_i=B_i=C_i$, so that

$$\frac{dA_i}{d\tau} = r^{kinet} \left(\Delta - 2 \frac{r^{therm}}{A_i} - \frac{r^{bal}}{r^{kinet} J} \right) = 2r^{kinet} r^{therm} \left(\frac{\Delta - \frac{r^{bal}}{r^{kinet} J}}{2r^{therm}} - \frac{1}{A_i} \right) \quad (20)$$

Actually, now we have the famous ‘‘Hillert-like’’ [6] (Lifshitz-Slezov type [7,8] but without extra A in the denominator) scheme of grain growth, with effective supersaturation

$$\Delta - \frac{r^{bal}}{r^{kinet} J},$$

$$Acrit = \langle A^2 \rangle / \langle A \rangle = \frac{2r^{therm}}{\Delta - \frac{r^{bal}}{r^{kinet} J}} \quad (21)$$

In asymptotics of long time it naturally gives supersaturation tending to $\frac{r^{bal}}{r^{kinet} J}$ instead of zero, and $Acrit$ proportional to the square root of time,

$$Acrit = (r^{kinet} r^{therm} \tau)^{1/2}.$$

Respectively, mean volume of one particle in symmetric case grows with time as $t^{3/2}$. – This is an important exponent, and we will come back to it below!

In the anisotropic case the supersaturation cannot simultaneously tend to $\frac{r_a^{bal}}{r_a^{kinet} J}, \frac{r_b^{bal}}{r_b^{kinet} J}$ and to $\frac{r_c^{bal}}{r_c^{kinet} J}$. Let, at first, consider the ‘‘partially symmetric’’ case when all ‘‘b-parameters’’ are equal to ‘‘c-parameters’’ (square section of nanofiber), and

$$\frac{r_a^{bal}}{r_a^{kinet}} < \frac{r_b^{bal}}{r_b^{kinet}} = \frac{r_c^{bal}}{r_c^{kinet}}$$

Then

$$\begin{aligned} \frac{dA_i}{d\tau} &= r_a^{kinet} \left(\Delta - \frac{2r_b^{therm}}{B_i} - \frac{r_a^{bal}}{r_a^{kinet} J} \right) \\ \frac{dB_i}{d\tau} &= r_b^{kinet} \left(\Delta - \frac{r_a^{therm}}{A_i} - \frac{r_b^{therm}}{B_i} - \frac{r_b^{bal}}{r_b^{kinet} J} \right) \end{aligned} \quad (22)$$

At the late ripening stage supersaturation should tend to $\frac{r_b^{bal}}{r_b^{kinet} J}$, mean values $\langle A \rangle$ and $\langle B \rangle$ should tend to infinity (but according to different time laws) and the total volume should tend to constant value:

$$\sum A_i B_i^2 = const \Rightarrow \sum (B_i^2 \frac{dA_i}{d\tau} + 2A_i B_i \frac{dB_i}{d\tau}) = 0 \quad (23)$$

$$\begin{aligned}\frac{dA_i}{d\tau} &\approx r_a^{kinet} \left(\frac{r_b^{bal}}{r_b^{kinet}} - \frac{r_a^{bal}}{r_a^{kinet}} \right) J \Rightarrow \langle A \rangle \approx r_a^{kinet} \left(\frac{r_b^{bal}}{r_b^{kinet}} - \frac{r_a^{bal}}{r_a^{kinet}} \right) J \tau = V \tau \\ \frac{dB_i}{d\tau} &= r_b^{kinet} \left(\left(\Delta - \frac{r_b^{bal}}{r_b^{kinet}} J \right) - \frac{r_a^{therm}}{A_i} - \frac{r_b^{therm}}{B_i} \right) \approx r_b^{kinet} \left(\left(\Delta - \frac{r_b^{bal}}{r_b^{kinet}} J \right) - \frac{r_b^{therm}}{B_i} \right)\end{aligned}\quad (24a,b)$$

$$\Sigma(B_i^2 r_a^{kinet} \left(\frac{r_b^{bal}}{r_b^{kinet}} - \frac{r_a^{bal}}{r_a^{kinet}} \right) J + 2 r_b^{kinet} \left(\left(\Delta - \frac{r_b^{bal}}{r_b^{kinet}} J \right) A_i B_i - r_b^{therm} A_i \right)) \approx 0 \quad (25)$$

According to approximate eqs. (24), statistically A and B, in the late ripening stage, are not correlated, so that $\langle AB \rangle = \langle A \rangle \langle B \rangle$

$$\begin{aligned}r_a^{kinet} \left(\frac{r_b^{bal}}{r_b^{kinet}} - \frac{r_a^{bal}}{r_a^{kinet}} \right) J * \langle (B^2) \rangle + \\ 2 r_b^{kinet} \langle A \rangle \langle B \rangle \left(\left(\Delta - \frac{r_b^{bal}}{r_b^{kinet}} J \right) - \frac{r_b^{therm}}{\langle B \rangle} \right) \approx 0\end{aligned}\quad (26)$$

$$\begin{aligned}\Delta - \frac{r_b^{bal}}{r_b^{kinet}} J \approx \frac{r_b^{therm}}{\langle B \rangle} - \frac{r_a^{kinet} \left(\frac{r_b^{bal}}{r_b^{kinet}} - \frac{r_a^{bal}}{r_a^{kinet}} \right) J}{2 r_b^{kinet}} \frac{\langle B^2 \rangle}{\langle B \rangle \langle A \rangle} \approx \\ \approx \frac{1}{\langle B \rangle} \left(r_b^{therm} - \frac{\langle B^2 \rangle}{2 r_b^{kinet} \tau} \right)\end{aligned}\quad (27)$$

Thus,

$$\frac{dB_i}{d\tau} \approx r_b^{kinet} r_b^{therm} \left(\frac{1}{B_{cr}} - \frac{1}{B_i} \right), \quad (28)$$

with

$$B_{cr} = \frac{\langle B \rangle}{1 - \frac{\langle B^2 \rangle}{2 r_b^{therm} r_b^{kinet} \tau}} \quad (29)$$

Anybody may check by direct calculations that the solution of equation for size distribution

$$\begin{aligned}\frac{\partial f(\tau, A, B)}{\partial \tau} &= -\frac{\partial}{\partial A} \left(f \frac{dA}{d\tau} \right) - \frac{\partial}{\partial B} \left(f \frac{dB}{d\tau} \right) = \\ &= -V \frac{\partial f}{\partial A} - r^{kinet} r^{therm} \frac{\partial}{\partial \rho} \left(\left(\frac{1}{B_{crit}} - \frac{1}{B} \right) f \right),\end{aligned}\quad (30)$$

with

$$V = r_a^{kinet} \left(\frac{r_b^{bal}}{r_b^{kinet}} - \frac{r_a^{bal}}{r_a^{kinet}} \right) J, \quad (31)$$

and with account of matter conservation in ripening, has the following explicit form:

$$f(\tau, A, B) = \text{const} \cdot \tau^{-5/2} \cdot \varphi(A - V\tau) \cdot \frac{(B/B_{crit})^1}{(2 - B/B_{crit})^6} \exp\left(\frac{-4B/B_{crit}}{2 - B/B_{crit}}\right),$$

$$\langle B \rangle = \frac{13}{16} B_{crit}, \quad \langle B^2 \rangle = \frac{3}{4} B_{crit}^2, \quad \langle B/B_{crit} \rangle = 1 - \frac{1}{4} \langle (B/B_{crit})^2 \rangle, \quad (32)$$

$$B_{crit} = \sqrt{\frac{1}{2} r_b^{kinet} r_b^{therm} \tau}$$

Distribution (32) includes linear (proportional to time) growth law for one crystallographic direction, and much more slower parabolic (proportional to square root of time) growth law for lateral sizes – so, it predicts formation of fibers with aspect ratio (lateral size to longitudinal) tending to zero.

For more general case, $\frac{r_a^{bal}}{r_a^{kinet}} < \frac{r_b^{bal}}{r_b^{kinet}} < \frac{r_c^{bal}}{r_c^{kinet}}$, so far, we don't have analytical solution, we have only first numeric results – they will be discussed elsewhere, after varying the main parameters, systematic study and doublechecking.

4. Preliminary conclusions

1. Process of V₂O₅ nanobelts production is drastically accelerated by intensive stirring which provides (1) higher (non-equilibrium) concentration of VO₃⁻ and VO₂⁺ ions in water, (2) faster ions transfer between facets of the same and of different particles, (3) additional ballistic (non-Arrhenius, athermal) erosion – anisotropic detachments from different facets.
2. Mechanism of “squeezing” of nanobelts from the nonequilibrium initial particles (by analogy with tin whisker growth from the tin stressed thin film via the “holes” in native oxide), so far, seems to be unlikely.
3. If one assumes that the facets of nanobelts remain atomically flat during growth, then the “layer-by-layer”, nucleation-controlled growth mechanism could really provide preferential growth in one direction due to strong anisotropy of the nucleation barrier of 2D-islands of new layer at different facets.
4. In the conditions of intensive stirring, the atom-by-atom growth mechanism (with attachments to the kinks of non-ideal facets) seems to be more likely.
5. Processes of redistribution between different particles and between different facets of the same particle are very complicated. In this paper we consider only simplest model of such redistribution (adding of ballistic detachment rates). Such modification, in the isotropic case, would just redefine an effective supersaturation. In anisotropic case, when ballistic terms are different at different facets, they lead to a much more interesting behavior.
6. As shown recently [3], at nucleation stage of the anisotropic particles, even if stochastic terms are switched off, the size space contains 3 regions: (1) absolutely unstable (embryo shrinks in volume to zero at any kinetic coefficients), (2) absolutely stable (nuclei increase their volume at any kinetic coefficients) and (3) transient region, in which the fate of the particle is determined but the set of kinetic coefficients. Stirring shifts the boundaries of these regions and even may make the nucleation impossible.
7. At advanced ripening stages, at least in partially symmetric case (a \approx b = c) the mean length tends to infinity linearly with time, the mean cross-section size grows parabolically, and the aspect ratio tends to infinity.
8. Detailed study of size and shape distributions evolution is still needed, at various concentrations of NaCl, at various temperatures etc.

References

- [1] X. Rui, Y.Tang, O.I. Malyi, A. Gusak, Y. Zhang, Z. Niu, ... Q.Yan. *Nano Energy*, 22 (2016), 583-593.
- [2] A. Gusak, Y. Huriev, O.I. Malyi, Y.Tang. *Physical Chemistry Chemical Physics*, 22 (2020), 9740-9748.
- [3] A. Gusak, Y. Huriev, J.W.Schmelzer. *Entropy*, 22/11 (2020), 1254.
- [4] A.M. Gusak, Y.I. Huriev, D.S. Gertsricken. *Cherkasy University Bulletin: Physical and Mathematical Sciences*, 1 (2021), 3-16.
- [5] G.Martin, *Physical Review B*, 30(3), (1984) 1424.
- [6] Hillert, M. (1965). On the theory of normal and abnormal grain growth. *Acta metallurgica*, 13(3), (1965) 227-238.
- [7] I. M. Lifshitz, V. V. Slyozov, *J. Phys. Chem. Solids* 19 (1961) 35–50.
- [8] V.V, Slezov. *Kinetics of first order phase transitions*. John Wiley & Sons, 2009.